CrystEngComm

Accepted Manuscript

ROYAL SOCIETY OF CHEMISTRY

www.rsc.org/crystengcomm

Interplay between hydrogen bonding and metal coordination in alkali metal tartrates and hydrogen tartrates

Thomas Gelbrich, Terence L. Threlfall and Michael B. Hursthouse

The aggregation of tartaric acid anions in the solid state is based on a small set of standard O–H···O bond motifs.

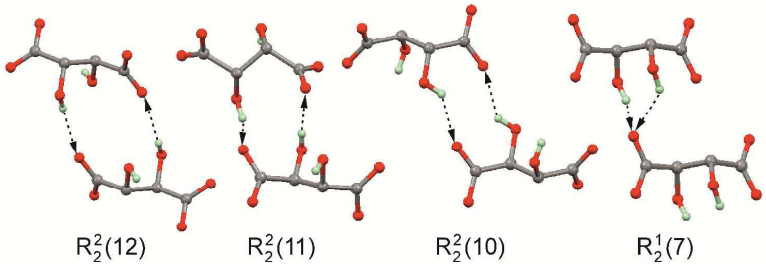

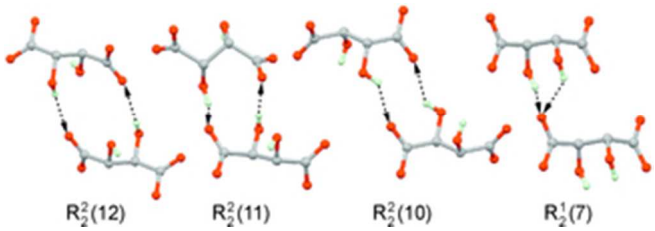

27x9mm (300 x 300 DPI)

Interplay between hydrogen bonding and metal coordination in alkali metal tartrates and hydrogen tartrates

Thomas Gelbrich,*[a] Terence L. Threlfall[b] and Michael B. Hursthouse[b,c]

Received (in XXX, XXX) Xth XXXXXXXXX 2014, Accepted Xth XXXXXXXXX 2014
First published on the web Xth XXXXXXXXX 2014
DOI: 10.1039/b000000x

The reactions of D,L-tartaric acid (D,L-H_2Tart) with alkali metal hydroxides *M*OH (*M* = Li, Na, Rb, Cs) in aqueous solution yielded new polymorphs of Na(D,L-HTart)·H_2O (**1a**) and Cs(D,L-HTart) (**2a**) as well as crystals of LiCs(D,L-Tart)·$2H_2O$ (**3**) and the conglomerate $(Rb_{0.5}Cs_{0.5})_2$(D-Tart) (**4**) / $(Rb_{0.5}Cs_{0.5})_2$(L-Tart). The crystal structures of these salts display 1D (**1a**, **2a**), 2D (**3**) or 3D (**4**) coordination polymers in combination with a hydrogen bonded layer (**1a**), framework (**2a**, **4**) or tape (**3**) structure. The triclinic and monclinic polymorphs of Na(D,L-HTart) · H_2O (**1**) exhibit a close one-dimensional packing similarity. Standard O–H···O=C hydrogen bond motifs for the aggregation $HTart^-$ and $Tart^{2-}$ ions in the solid state were identified from a comparison involving 35 crystal structures of chiral and racemic *M*HTart and M_2Tart salts (*M* = alkali metal).

Introduction

As part of a wider study of the aggregation patterns of tartrate ($Tart^{2-}$) and hydrogen tartrate ($HTart^-$) ions in the solid state, we are investigating the salts formed by reactions between alkali metal (*M*) hydroxides (*M*OH) or NH_4OH and D,L-tartaric acid (Scheme 1) in a well plate screening experiment. We have previously reported[1] a series of isostructural salts of the formula *M*(D,L-HTart) with *M* = K (**5**), Rb (**6**), Cs (**2b**), NH_4, Li_2(D,L-Tart) · $3H_2O$ (**7**), LiNa(D,L-Tart) · $2H_2O$ (**8**) and the series Li*M*(D,L-Tart) · H_2O with *M* = K, Rb, Cs (**9** – **11**), NH_4). These crystals may be described as coordination polymer networks in which the organic ions serve as linkers between alkali metal centres and where the anions and water molecules (if present) are additionally connected to one another by classical hydrogen bonds.

Coordination polymers[2] have been widely studied, and their structural characteristics can be tailored for various potential applications including gas storage[3] and separations,[4] catalysis[5] and luminescence.[6] However, the application of crystal engineering design strategies[7] for coordination networks of groups 1 and 2 metal ions is hampered by a lack of predictability and control over coordination geometries.[8] At the same time, the tartrate and hydrogen tartrate species offer, and usually adopt, more flexible linking patterns, with the added possibility of chirality, than do the typical ligands used in MOF chemistry. Accordingly an "information gathering process", *via* a systematic crystallisation and structure determination process, is required to establish the chemical and structural landscape.

Here we report new polymorphs of Na(D,L-HTart) · H_2O (**1**) and Cs(D,L-HTart) (**2**) as well as the bis-metal tartrate dihydrate LiCs(D,L-Tart) · $2H_2O$ (**3**) and the mixed crystal $(Rb_{0.5}Cs_{0.5})_2$(D-Tart) (**4**). The structural characteristics of these crystals will be compared to those of the other known racemic and chiral *M*HTart and M_2Tart salts in order to identify packing relationships and common patterns of hydrogen bonding interactions.

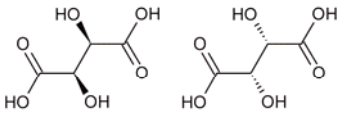

D,L-tartaric acid (D,L-H_2Tart)

Scheme 1

Experimental

Preparation

Aqueous solutions (0.2 molar) of D,L-H_2Tart and the hydroxides *M*OH (*M* = Li – Cs, NH_4) were used for all preparations. Different mixtures of these components were prepared in the wells of a 96 well plate, using a liquid handling robot. The identity of the crystalline phases formed from these mixtures was established by single crystal X-ray diffraction. Several new crystal structures obtained from these room temperature experiments have been reported in previous accounts (see above).[1] An overview of all crystallisation experiments and identified phases is given in Table S7 (ESI).† Single crystals of Na(D,L-HTart) · H_2O (**1a**) were obtained from a 1:1 mixture of D,L-H_2Tart and NaOH after one week. The 1:1 mixture of D,L-H_2Tart and CsOH yielded the triclinic polymorph of Cs(D,L-HTart) (**2a**) after one week.

Two distinct phases, the dihydrate LiCs(D,L-Tart) · $2H_2O$ (**3**) and a previously reported monohydrate (**11**),[1b] were obtained from the 1:1:1 solution mixture of LiOH, CsOH and D,L-

H_2Tart after three weeks.

The investigated crystal of $(Rb_{0.5}Cs_{0.5})_2$(D-Tart) (**4**) was contained in the racemic conglomerate obtained from the reaction of a 1:1:1 mixture of D,L-H_2Tart, CsOH and RbOH after three weeks.

X-ray crystallography

Intensity data were recorded on a Nonius KappaCCD diffractometer situated at the window of a Bruker Nonius FR591 rotating anode generator equipped with a Mo target (λ = 0.71073 Å) and driven by COLLECT[9], DirAx[10] and DENZO[11] software, and the data were corrected for absorption effects by means of comparison of equivalent reflections using the program SADABS.[12] Crystallographic parameters for **1a**, **2a**, **3** and **4** are collected in Table 1. The structures were solved using the direct methods procedure in SHELXS97 and refined by full-matrix least squares on F^2 using SHELXL97.[13] Non-hydrogen atoms were refined anisotropically. Hydrogen atoms in CH groups, although located easily in difference maps, were fixed in idealised positions, as were the H atoms in the hydroxyl groups of **1a** and **2a**. Water hydrogen atoms were refined with O–H bond lengths restrained to 0.86(1) Å and the H···H distance restrained to 1.36(2) Å. The H atoms of the hydroxyl groups of **2a** and **4** were refined with O–H bond lengths restrained to 0.84(1) Å. The U_{iso}(H) parameters of H atoms in the CH and hydroxyl groups of **1a** and **3** were refined with U_{iso}(H) = 1.2 U_{eq}(C,O), and all other U_{iso}(H) parameters were refined freely.

The investigated crystal of **4** showed combined merohedral and racemic twining, and the latter indicates the presence of the D and L-forms in a ratio of 84:16. The introduction of the merohedral twin matrix $[\bar{1}00\ 0\bar{1}0\ 001]$ into the structure refinement reduced wR2 (for all data) from 0.543 to 0.063 and the ratio of the corresponding merohedral twin components was 60:40. The refinement of the split metal atom position indicated a 1:1 occupancy of Rb and Cs.

Analysis of crystal structures

XPac studies. Crystal packing comparisons were carried out using the program *XPac*[14] and quantitative dissimilarity parameters were generated in the previously described[15] manner.‡ All comparisons were based on geometrical parameters generated from the C and O atoms of the anion, whereas metal centres and water molecules were not considered.

H-bond topology. The classification of the hydrogen bonded networks was carried out with the *ADS* and *IsoTest* routines of the TOPOS package[16] in the manner described by Baburin & Blatov.[17]

Table 1. Crystallographic parameters and details of the structure determinations.

	1a	**2a**	**3**	**4**
Compound	Na(D,L-HTart) · H_2O	Cs(D,L-HTart)	CsLi(D,L-Tart) · $2H_2O$	$(Rb_{0.5}Cs_{0.5})_2$(D-Tart)
Chemical formula	$C_4H_7NaO_7$	$C_4H_5CsO_6$	$C_4H_8CsLiO_8$	$C_4H_4CsO_6Rb$
Formula mass	190.09	281.99	323.95	366.45
Crystal system	triclinic	triclinic	monoclinic	trigonal
Space group	$P\bar{1}$	$P\bar{1}$	$P2_1/c$	$P3_121$
Z	2	2	4	3
a/Å	6.4939(17)	5.0645(3)	5.0731(3)	7.2835(5)
b/Å	7.0655(11)	7.2545(5)	16.9391(12)	7.2835(5)
c/Å	7.978(2)	9.9570(6)	10.5094(9)	13.2453(7)
α/°	91.640(16)	72.369(4)	90	90
β/°	101.564(9)	85.460(4)	98.777(2)	90
γ/°	110.577(14)	85.837(3)	90	120
Unit cell volume/Å^3	333.79(13)	347.09(4)	892.54(11)	608.52(7)
Temperature/K	120(2)	120(2)	120(2)	120(2)
No. of reflections measured	1779	2549	5023	6141
No. of independent reflections	1086	1309	1701	882
R_{int}	0.0428	0.0429	0.0613	0.0739
Final R_1 values ($I > 2\sigma(I)$)	0.0477	0.0288	0.0394	0.0259
Final $wR(F^2)$ values (all data)	0.1124	0.0707	0.0782	0.0627

Results and discussion

The method of crystallisation applied in this study naturally produced very small quantities of solids (only one or two crystals in some cases) and additionally some of the crystallisation experiments yielded multiple phases (Table S7, ESI†). Our aim was to explore what phases could be obtained, what their structures were and how they were related. The whole thrust of the work was to "discover" new forms, and engage in a structural systematics analysis, whereas the investigation of bulk properties was not part of this investigation.

Triclinic polymorph of Na(D,L-HTart) · H_2O (1a)

The asymmetric unit of **1a** contains one formula unit. Each Na^+ ion is coordinated by one water molecule and four $HTart^-$ ligands, and two of the latter are chelating (Fig. 1a). Each $HTart^-$ ligand is bonded to four different Na^+ ions *via* one hydroxyl oxygen atom and three unprotonated carboxylic oxygen atoms and may be described as μ_4, κ^4. The seven-fold Na^+ coordination is formed by three hydroxyl and three

carboxyl oxygen atoms of $HTart^-$ and the water molecule. The Na–O distances lie between 2.38 and 2.60 Å (Table 2) and the sodium coordination geometry is a capped trigonal prism. Edge-sharing NaO_7 polyhedra are linked into infinite chains which propagate along [010] and display two independent Na_2O_2 rings, with the shortest Na···Na separations being 3.62 and 3.98 Å (Fig. 1b). Overall, Na^+ ions and D,L-$HTart^-$ ligands form a 2D coordination network which lies parallel to the (001) plane (Fig. 1c).

$HTart^-$ ions and water molecules are linked into a 2D H-bonded net which propagates parallel to the (100) plane (Fig. 1d). The hydrogen bond donor functions of the three hydroxyl groups of $HTart^-$ (*t*) and the water molecule (*w*) are employed in these interactions (Table 3). Head-to-tail interactions (*t*)O–H···O(*t*) involving the hydrogen atom of the protonated carboxyl oxygen atom generate the chain denoted A-*syn* in Fig. 2b. Two chains of this kind are linked, *via* a second (*t*)O–H···O(*t*) interaction, into a ladder structure (Fig. 2c), which lies parallel to the *b*-axis. It displays two kinds of fused centrosymmetric rings having the graph set[18] symbols $R_2^2(12)$ and $R_4^4(18)$. Bridging water molecules connect neighbouring ladder structures to one another *via* one (*t*)O–H···O(*w*) and two (*w*)O–H···O(*t*) interactions (Table 3). Altogether, $HTart^-$ ions and water molecules form a 2D hydrogen bonded structure parallel to the (100) plane (Fig. 2d). Each metal centre is coordinated by oxygen atoms originating from two such hydrogen bonded layers so that the combination of coordination network and hydrogen bonding results in a framework structure.

Table 2. Selected geometrical parameters (Å) for **1a**, **2a** and **3** (longer *M*–O contacts are indicated by an asterisk and drawn as dotted lines in Figs. 3a and 4a).

Na (D,L-HTart) · H_2O (**1a**)	
Na1–O4^{i}	2.382(2)
Na1–O7	2.419(2)
Na1–O1	2.437(2)
Na1–O3^{ii}	2.474(2)
Na1–O1^{iii}	2.478(2)
Na1–O3^{iii}	2.532(3)
Na1–O5^{i}	2.599(2)
Cs(D,L-HTart) (**2a**)	
Cs1–O2^{i}	3.067(2)
Cs1–O4^{ii}	3.093(3)
Cs1–O6^{iii}	3.129(3)
Cs1–O3	3.195(3)
Cs1–O5^{iv}	3.214(3)
Cs1–O2^{v}	3.294(3)
Cs1–O1^{ii}	3.348(3)
Cs1–O1^{vi}	3.352(2)
Cs1–O6	3.457(3)
Cs1–O1^{v}	3.586(3)*
Cs1–O5	3.717(3)*
CsLi(D,L-Tart) · $2H_2O$ (**3**)	
Cs1–O7^{i}	3.076(4)
Cs1–O6^{ii}	3.078(4)
Cs1–O2^{iii}	3.131(3)
Cs1–O3^{ii}	3.163(3)
Cs1–O8^{iv}	3.272(4)
Cs1–O5^{i}	3.332(4)
Cs1–O1	3.338(4)
Cs1–O8^{i}	3.484(4)
Cs1–O5^{ii}	3.533(4)
Cs1–O8^{ii}	3.629(4)*
Cs1–O2	3.636(4)*
Cs1–O7^{iv}	3.731(3)*
Li1–O5^{v}	1.882(10)
Li1–O6	1.927(11)
Li1–O8	1.930(10)
Li1–O7	1.964(10)

Symmetry transformations used to generate equivalent atoms:
1a: (i) $-x+1, -y+1, -z+2$ (ii) $x, y+1, z$ (iii) $-x, -y+1, -z+2$.
2a: (i) $x-1, y-1, z$ (ii) $x, y-1, z$ (iii) $x-1, y, z$ (iv) $-x, -y, -z+2$ (v) $-x+1, -y+1, -z+1$ (vi) $-x, -y+1, -z+1$. **3**: (i) $-x+1, y+1/2, -z+3/2$ (ii) $-x+1, -y+1, -z+1$ (iii) $x, -y+3/2, z-1/2$ (iv) $-x+2, y+1/2, -z+3/2$ (v) $x+1, y, z$ (viii, Fig. 4) $-x, y+1/2, -z+3/2$.

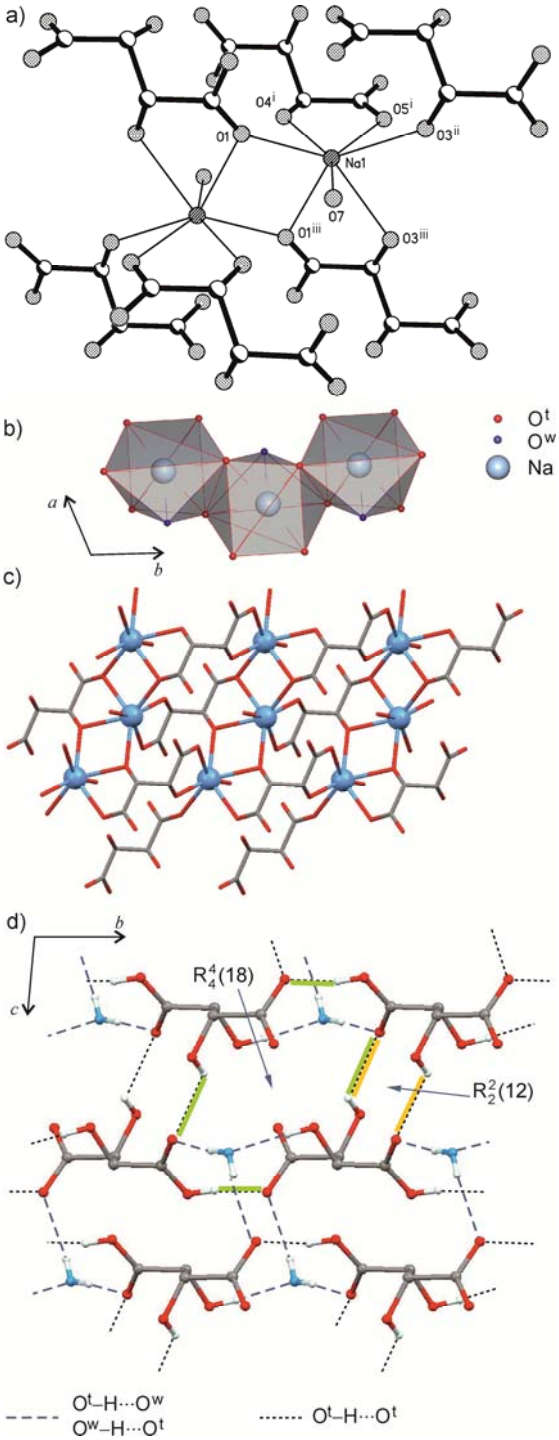

Fig. 1 Crystal structure of **1a**. a) Coordination of Na^+ by four $HTart^-$ ions and one water molecule (O7); for symmetry operations, see Table 2; b) chain of edge-sharing NaO_7 polyhedra; c) 2D coordination network parallel to (001), composed of Na^+ ions (balls) and $HTart^-$ ligands (rods; H atoms are omitted for clarity); d) 2D hydrogen bonded network composed of $HTart^-$ ions and water molecules (view along [100]; H atoms not participating in hydrogen bonding are omitted for clarity).

A monoclinic modification (**1b**) of Na(D,L-HTart) · H_2O, obtained from the reaction of D,L-H_2Tart and $NaHCO_3$ in aqueous solution under reflux and subsequent cooling of the solution under stirring, was reported by Al-Dajani *et al.*[19] The *XPac* comparison of the $HTart^-$ substructures present in **1a** and **1b** revealed a centrosymmetric hydrogen bonded double-stranded chain structure (Fig. 2c) as a common supramolecular construct[14] (SC) of the two polymorphs. In both polymorphs the ladder units propagate parallel to the *b*-axis (**1a**: 7.065 Å; **1b**: 7.146 Å), and their geometrical closeness is evidenced by a low *XPac* dissimilarity index,[15] x = 2.2 (calculated for a cluster of five connected $HTart^-$ ligands defining this SC; for the definition of x and reference examples, see refs. 15 and 20).

However, the forms **1a** and **1b** differ fundamentally in the mode by which neighbouring ladder units are linked by water molecules into an H-bonded layer structure (Fig. 2d, e). In **1a**, each water molecule bridges between two ladder units that are related by an inversion operation, whereas **1b** it connects two such units related by a 2_1 screw operation. Therefore, the two polymorphs of Na(D,L-HTart) · H_2O exhibit a close 1D packing relationship. The density of polymorph **1a** (1.891 g cm^{-3}) is only 0.4% higher than that of **1b** (1.884 g cm^{-3}).

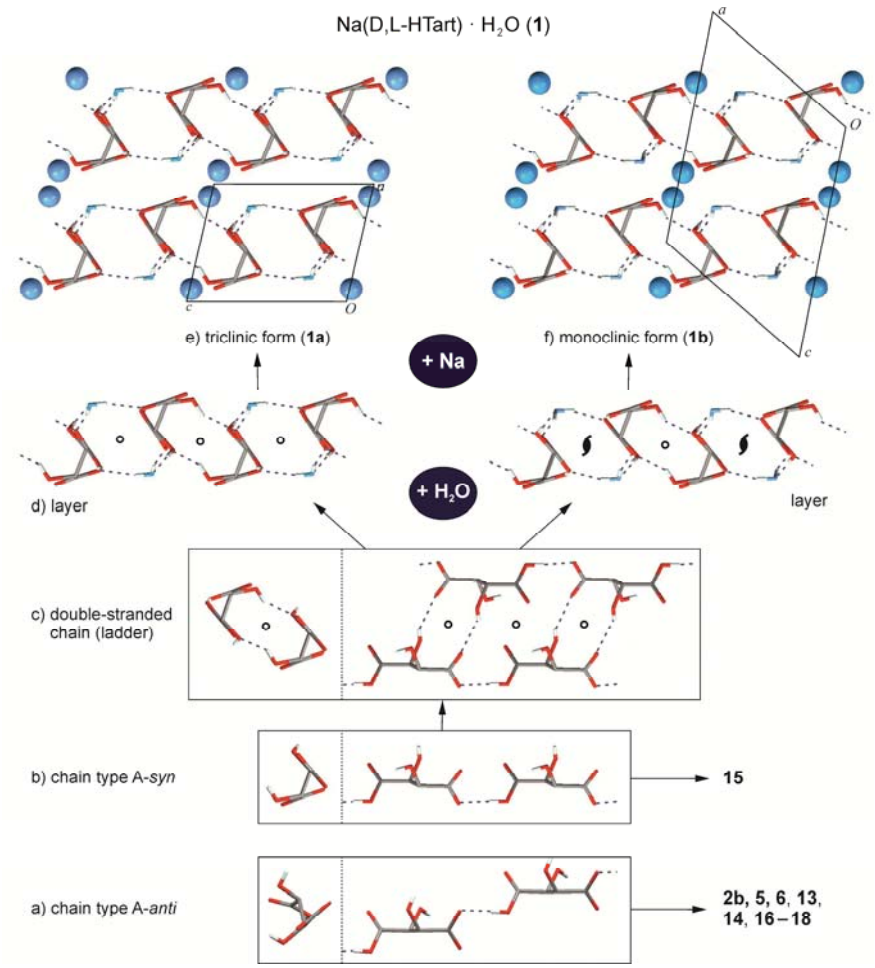

Fig. 2 Alternate chain types A-*anti* (a) and A-*syn* (b) formed by O−H···O bonded $HTart^-$ ions, each viewed parallel (left) and perpendicular (right) to the translation vector of the chain; c) ladder structure composed of two (*t*)O−H···O(*t*) connected A-*syn* strands, which displays fused $R_2^2(12)$ and $R_4^4(18)$ rings; d) layer structure composed of ladder units related either by inversion (**1a**) or 2_1 symmetry (**1b**) and linked to one another by H-bonded water molecules; packing of H-bonded $HTart^-$/water layers and Na^+ ions (drawn as balls) in the polymorphs **1a** (e) and **1b** (f).

Triclinic polymorph of Cs(D,L-HTart) (2a)

The three isostructural monoclinic hydrogen tartrates *M*(D,L-HTart) with *M* = K (**16**), Rb (**17**) and NH_4 were obtained from 1:1 mixtures of D,L-H_2Tart with the respective hydroxide *M*OH,[1a] while the analogous reaction with *M* = Cs resulted in the triclinic form of Cs(D,L-HTart) (**2a**). Furthermore, 1:1:1 mixtures of D,L-H_2Tart with any two hydroxides of KOH, RbOH and NH_4OH yielded the corresponding hydrogen tartrate mixed crystals, but no such mixed crystals were obtained from any of the analogous mixtures containing CsOH. Instead, the preparation of D,L-H_2Tart with CsOH and NH_4OH yielded a monoclinic form of Cs(D,L-HTart) (**2b**) as well as crystals of NH_4(D,L-HTart). Both these phases are isostructural with the analogous potassium (**16**) and rubidium (**17**) compounds (Table S7, ESI†).[1a]

The asymmetric unit of **2a** contains one Cs^+ and one $HTart^-$ ion. The Cs centre is surrounded by nine oxygen atoms belonging to seven different $HTart^-$ ligands (Fig. 3a) and the corresponding Cs–O separations range widely from 3.07 − 3.46 Å (Table 2). Each $HTart^-$ unit is attached to seven Cs^+ centres and all its oxygen atoms are engaged in Cs−O interactions (μ_7, κ^6). Two ligands chelate with one carboxyl and one hydroxyl oxygen atom and all other bonds are of the Cs−O(carboxyl) type. Each CsO_9 polyhedron shares a face with a neighbouring polyhedron and an edge with another one so that a chain of connected CsO_9 units is formed, which lies parallel to [001] (Fig. 3b). In addition to the Cs−O bonds mentioned above, there are two longer Cs−O contacts (3.59 Å, 3.72 Å; indicated by broken lines in Fig. 2a) which involve additional carboxyl O atoms of two coordinating $HTart^-$ units, and the shortest Cs···Cs distance in **2a** is 4.80 Å. The connected Cs^+ and $HTart^-$ ions form a framework structure.

The carboxyl hydrogen atom is 1:1 statistically disordered over two positions (O1 and O6), one in each carboxyl group. Each $HTart^-$ ligand is bonded to five other ligands via six O–H···O bonds to give a hydrogen bonded framework (Fig. 3c), whose topology is of the boron nitrite (bnn)[21] type. It

displays centrosymmetric $R_4^4(24)$ and $R_2^2(10)$ rings where the latter ring type is due to intermolecular interactions involving the deprotonated carboxyl group (O5) and the adjacent hydroxyl group (O4) of each $HTart^-$ ion as the H-bond acceptor and donor sites, respectively. The Cs^+ ions occupy the large cavities of this H-bonded framework.

Table 3. Geometrical parameters (Å, °) for hydrogen bonds.

D−H···*A*	*D*−H	D···*A*	H···*A*	∠ *D*−H···*A*
Na(D,L-HTart) · H_2O (**1a**)				
(*t*) O3−H3···O5^{ix} (*t*)	0.84	2.21	2.832(3)	130.9
(*t*) O2−H6···O6^{v} (*t*)	0.84	1.64	2.464(3)	167.8
(*t*) O4−H4···O7^{viii} (*w*)	0.84	1.86	2.686(3)	170.0
(*w*) O7−H8···O2^{vi} (*t*)	0.849(10)	2.027(12)	2.852(3)	164(4)
(*w*) O7−H7···O5^{vii} (*t*)	0.851(10)	1.898(12)	2.724(3)	163(3)
Cs(D,L-HTart) (**2a**)				
O1−H1···O1^{vii}	0.840(10)	1.65(3)	2.472(5)	166(11)
O3−H3O···O2^{iii}	0.836(10)	1.972(17)	2.778(3)	162(4)
O4−H4O···O5^{viii}	0.838(10)	2.21(3)	2.855(4)	133(4)
O6−H6···O6^{ix}	0.840(10)	1.63(3)	2.449(5)	166(12)
LiCs (D,L-Tart) · $2H_2O$ (**3**)				
(*t*) O3−H3···O1^{x} (*t*)	0.84	2.19	2.873(6)	138.2
(*t*) O4−H4···O6^{ix} (*t*)	0.84	1.94	2.744(5)	159.0
(*w*) O7−H1O···O2^{xi} (*t*)	0.822(10)	1.94(2)	2.737(6)	164(6)
(*w*) O7−H2O···O4^{xii} (*t*)	0.824(10)	1.914(13)	2.735(5)	174(6)
(*w*) O8−H3O···O1^{vii} (*t*)	0.824(10)	1.914(18)	2.725(5)	168(6)
(*w*) O8−H4O···O2^{vi} (*t*)	0.822(10)	2.02(2)	2.792(5)	157(4)
O3−H3···O1 (intra)	0.84	2.19	2.678(5)	117.0
$(Rb_{0.5}Cs_{0.5})_2$(D-Tart) (**4**)				
O3−H3···O2^{ix}	0.837(9)	2.37(10)	2.928(8)	125(10)
O3−H3···O2 (intra)	0.837(9)	2.18(10)	2.690(9)	119(9)

Symmetry transformations used to generate equivalent atoms:
1a: (v) $x, y+1, z$ (vi) $-x, -y+1, -z+1$ (vii) $x-1, y+1, z$ (vii) $x+1, y, z$ (ix) $-x+1, -y, -z+2$. **2a**: (iii) $x-1, y, z$ (vii) $-x+1, -y+2, -z+1$ (viii) $-x, -y+1, -z+2$ (ix) $-x+1, -y, -z+2$. **3**: (vi) $-x+2, y-1/2, -z+3/2$ (vii) $-x+1, y-1/2, -z+3/2$ (ix) $x-1, y, z$ (x) $-x, -y+1, -z+1$ (xi) $-x+2, -y+1, -z+2$ (xii) $-x+1, -y+1, -z+2$. **4**: (ix) $x-y+1, -y+1, -z+5/3$

The $HTart^-$ unit of the monoclinic form **2b** may be described as μ_7, κ^5, and each Cs^+ centre in this structure is surrounded by eight oxygen atoms in a square-antiprismatic fashion with Cs−O distances of 3.02 − 3.27 Å (average 3.12 Å). There is just one additional Cs−O contact (3.67 Å) shorter than 4 Å. In comparison, the eight shortest Cs−O bonds (3.07 − 3.35 Å) of 3.21 Å of **2a** are significantly longer, which is offset by the presence of three additional Cs−O contacts up to 3.72 Å. The coordination polymers of both polymorphs are frameworks. However, the crystal of **2b** contains layers of Cs^+ ions which alternate with two types of hydrogen bonded layers composed exclusively of either D- or L-$HTart^-$ ions (Fig. S9†). This arrangement appears to be less efficient and is significantly less dense (2.613 g cm^{-3}) than the accommodation of Cs^+ ions within the H-bonded framework of the triclinic form **2a** (2.698 g cm^{-3}; difference 3%).

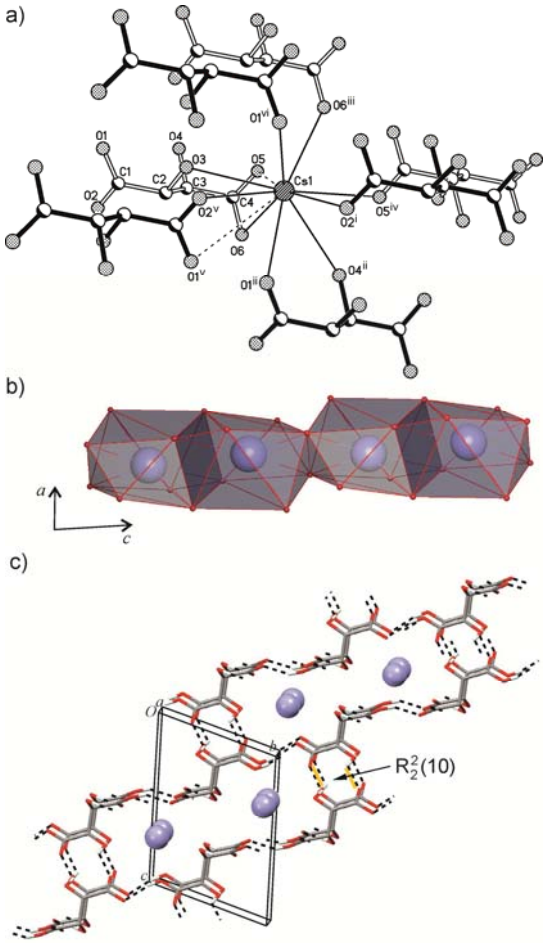

Fig. 3 Crystal structure of **2a**. a) The coordination of Cs^+ by seven $HTart^-$ ligands (for symmetry operations, see Table 2) resulting in nine shorter (full lines) and two longer (dashed lines) Cs−O distances; b) chain of connected edge-and face-sharing CsO_9 polyhedra parallel to [001]; c) framework of hydrogen bonded $HTart^-$ ions, with open channels occupied by Cs^+ (drawn as balls).

LiCs(D,L-Tart) · $2H_2O$ (3)

A series of analogous reactions yielded the previously reported[1b] isostructural compounds Li*M*(D,L-Tart) · H_2O [*M* = K, Rb, Cs (**9** – **11**), NH_4]. Additionally, the Cs dihydrate (**3**) was obtained with the monohydrate (**11**). The asymmetric unit of **3** contains one formula unit. The Cs^+ centre is surrounded by nine oxygen atoms with Cs−O distances between 3.08 and 3.53 Å and by another three oxygen atoms with longer Cs−O distances up to 3.73 Å (Table 2). The nine shortest Cs−O interactions involve one chelating $Tart^{2-}$ ion that is bonded *via* one hydroxyl and two carboxyl oxygen atoms, another three $Tart^{2-}$ ligands bonded *via* a carboxyl oxygen atom each and three water molecules (Fig. 4a). The tetrahedral coordination environment of Li^+ is formed by two carboxyl oxygen atoms belonging to different $Tart^{2-}$ ions and two water ligands. The tetrahedron around Li^+ is somewhat distorted with O−Li−O angles between 102.7° and 118.5°. The ligand connects to six different metal centres via five oxygen atoms and may therefore be described as μ_6, κ^5.

Corner-sharing LiO_4 and CsO_9 polyhedra form a 2D net which

lies parallel to the *ac*-plane (Fig. 4b). The $Tart^{2-}$ and metal ions are linked into a 3D coordination network. $Tart^{2-}$ units are connected by Cs centres within (100) planes and each Li^+ ion bridges between two $Tart^{2-}$ ions which are related by a translation along the *a*-axis.

The $Tart^{2-}$ anions are hydrogen bonded to one another *via* two hydroxyl donor and two carbonyl acceptor functions (Table 3). This generates an H-bonded 1D ladder structure parallel to [100] which exhibits centrosymmetric fused $R_2^2(10)$ and $R_4^4(24)$ rings. Each water molecule serves as an additional bridge between two (*t*)O–H···O(*t*) bonded $Tart^{2-}$ ions (Fig. 4c).

An *XPac* comparison showed that the ladder geometry of the H-bonded $Tart^{2-}$ ions of **3** with its fused $R_2^2(10)$ and $R_4^4(24)$ rings is also present in the H-bonded framework of **2a** (Fig. 5). Furthermore, **2a** and **3** also display the same arrangement of these ladders into a layer structure, *i.e.* their anion substructures are 2D similar with matching *ac* planes (dissimilarity index[15] x = 3.4 for the cluster of 9 anions defining the supramolecular construct[14]). **2a** and **3** differ in their chemical composition and in the external H-bond connections of their common layer structure so that the *c*-axis of **3** is 0.55 Å longer and β is 4.2° smaller than the corresponding parameters of **2a**. By contrast, the difference in the length of the *a*-axis (direction of the H-bonded chain) between **2a** and **3** is very small (Table 1).

The monohydrate **11** contains two independent Cs^+ centres which are each surrounded by 10 O atoms (Cs1–O: 3.19 to 3.31 Å, mean value 3.22 Å; Cs2–O: 3.04 to 3.58 Å, mean value 3.26 Å). The average of the ten shortest Cs–O distances in **3** is significantly higher (3.30 Å), which is compensated for by the additional presence of two longer Cs–O contacts of 3.64 and 3.73 Å. The monohydrate and dihydrate structures of LiCs(D,L-Tart) (**11** and **3**) differ also fundamentally in their H-bonded framework structures, their coordination polymers and the structures of their connected LiO and CsO polyhedra (Table 5).

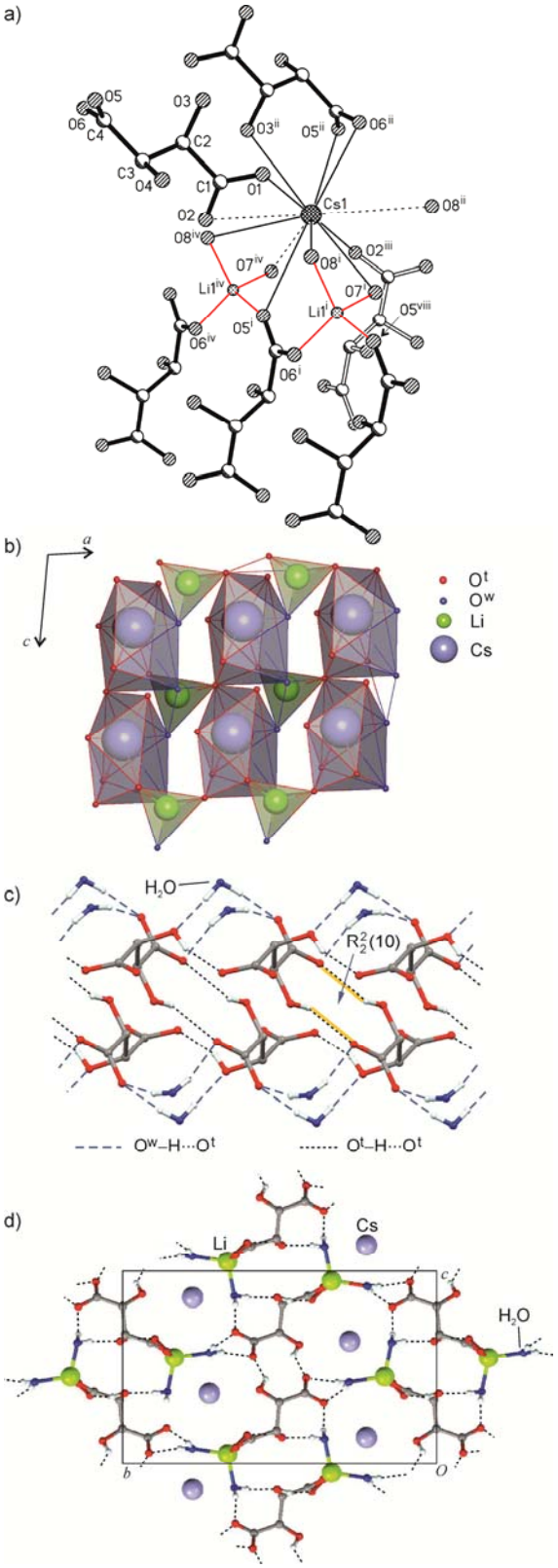

Fig. 4 Crystal structure of CsLi(D,L-Tart) · $2H_2O$ (**3**). a) Coordination environments of Cs^+ and Li^+ (O7 and O8 are water oxygen atoms; for symmetry operations, see Table 2); b) layer of connected corner-sharing LiO_4 and CsO_9 polyhedra; c) hydrogen bonded chain $[Tart^{2-} \cdot 2H_2O]_n$ propagating along [100]; d) crystal packing of H-bonded chains (which are O–Li–O linked to one another) and Cs^+ ions.

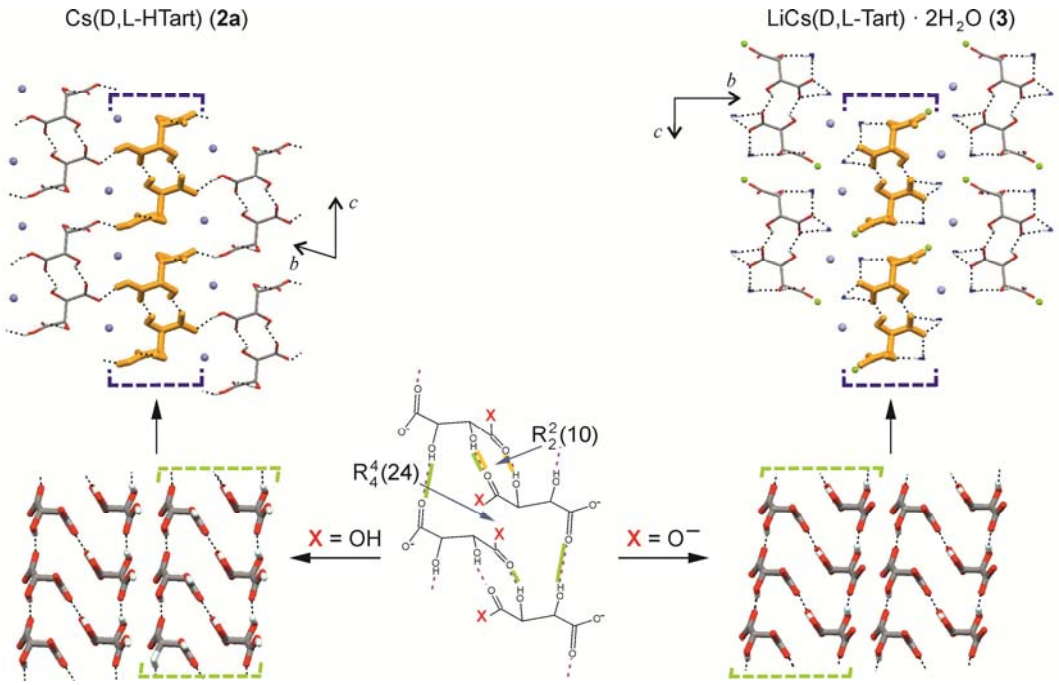

Fig. 5 2D packing similarity between Cs(D,L-HTart) (**2a**) and CsLi(D,L-Tart) · $2H_2O$ (**3**). Bottom: connectivity mode generating the common H-bonded ladder structure (centre) and the common 2D supramolecular construct. The structure fragments of **2a** (left) and **3** (right) are viewed along the *b**-axis, with the brackets indicating a single H-bonded chain. Top: the crystal structures of **2a** and **3**, viewed along the respective *a*-axis [Cs (light-blue), Li (green) and water O (dark-blue) atoms are represented as balls, H atoms are omitted for clarity, broken lines indicate H-bonds]; in each structure an instance of the 2D SC is highlighted and indicated by brackets.

$(Rb_{0.5}Cs_{0.5})_2$(D-Tart) (4)

The mixed crystal **4** is isostructural with its parent di-rubidium (**29**) and di-caesium compounds (**30**),[22] which differ in their unit cell volume by 11%. The unit cell parameters of **4** lie approximately half-way between those of **29** and **30**. The asymmetric unit of **4** consists of half a formula unit and the $Tart^-$ ion lies on a two-fold rotation axis and the site of the metal centre has a 1:1 mixed Cs/Rb occupancy. Each metal centre is surrounded by eight oxygen atoms belonging to six $Tart^{2-}$ units with (six *M*–O contacts are shorter 3.21 Å and eight are shorter than 3.45 Å), and there is an additional longer *M*–O contact of approximately 3.60 Å (Fig. 6a, Table 4). The ligand may be described as μ_{10}, κ^6 as each $Tart^{2-}$ ion is linked to ten metal sites and all hydroxyl and carbonyl oxygen atoms are engaged in metal coordination.

The $Tart^{2-}$ unit serves as a four-connected node within a O–H···O(carbonyl)-bonded framework structure (Fig. 6b) which has the quartz (qtz)[23] topology. Additionally, each OH group is also engaged in an intramolecular O–H···O(carbonyl) bond. Overall, the H-bond geometries of **4** appear to be less favourable than those found in **1**, **2a** and **3** (Table 3). The shortest circuit within the H-bonded framework of **4** is an $R_6^6(34)$ ring comprising six molecules. Both the $Tart^{2-}$ and metal ions are arranged around distinct 3_1 axes (Fig. 6c) and the M^+ ions are situated within the cavities of the framework of H-bonded anions.

Table 4. Selected geometrical parameters (Å) for **4**.

Cs1–O1^{i}	2.907(7)
Cs1–O1^{ii}	2.918(6)
Cs1–O1	3.016(5)
Cs1–O2^{iii}	3.043(5)
Cs1–O2^{iv}	3.084(6)
Cs1–O3^{v}	3.201(5)
Cs1–O3^{vi}	3.426(5)
Cs1–O2	3.439(6)
Cs1–O3^{vii}	3.568(8)*
Rb1–O1^{ii}	2.922(7)
Rb1–O1^{i}	2.929(9)
Rb1–O1	3.004(6)
Rb1–O2^{iii}	3.034(6)
Rb1–O2^{iv}	3.074(7)
Rb1–O3^{v}	3.188(7)
Rb1–O2	3.413(9)
Rb1–O3^{vi}	3.440(7)
Rb1–O3^{vii}	3.597(10)*

Symmetry transformations used to generate equivalent atoms:
(i) $-y+1, x-y+1, z+1/3$ (ii) $x-y+1, -y+2, -z+5/3$ (iii) $y, x, -z+2$ (iv) $x-y, -y+1, -z+5/3$ (v) $-y+1, x-y, z+1/3$ (vi) $x-1, y, z$ (vii) $x-y, -y+2, -z+5/3$

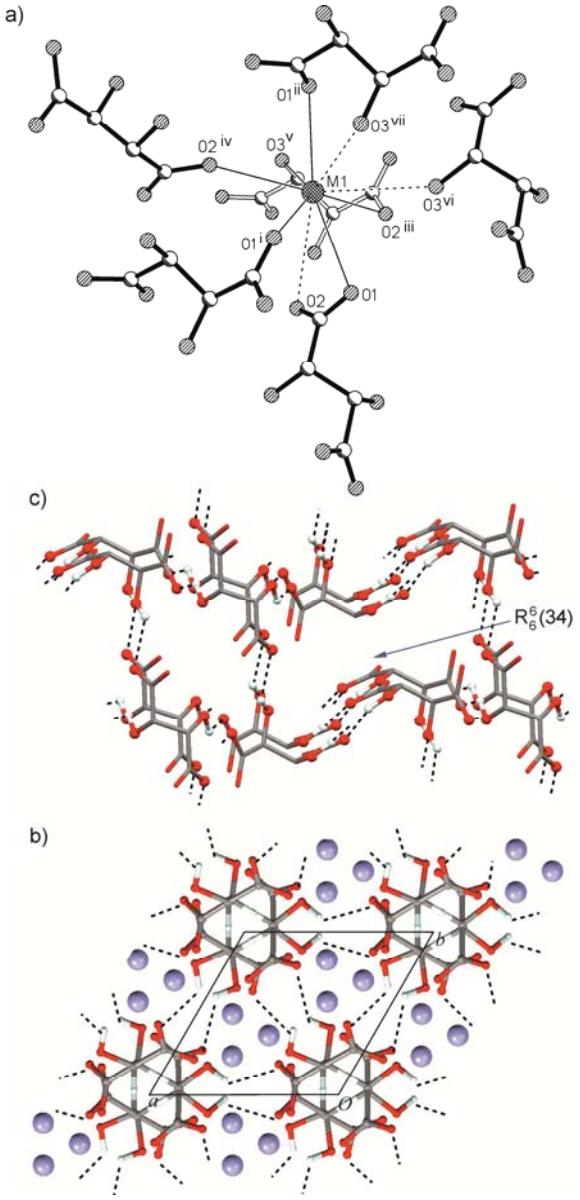

Fig. 6 a) Crystal structure of $(Rb_{0.5}Cs_{0.5})_2$(D-Tart) (**4**). a) Coordination environment of M = Rb or Cs (for symmetry operations, see Table 4); b) framework of H-bonded $Tart^{2-}$ ions with c) metal ions (balls) filling its cavities (intramolecular H-bonds are not shown)

Systematics *M*HTart and M_2Tart structures (M = alkali metal)

Important structural characteristics of **1a**, **2a**, **3** and **4** have been collected in Table 5, together with the features of 30 other chiral or racemic alkali metal tartrates or hydrogen tartrates from the Cambridge Structural Database[24] (CSD; version 5.33). The listed characteristics include the coordination number of metal centres (n), the number of metal centres attached to an anionic ligand (μ), the number of coordinating O atoms per ligand (κ), the dimensionality of the extended structure consisting of connected MO_n polyhedra, the dimensionality of the coordination polymer and the dimensionality of the hydrogen-bonded structure of anions and (if applicable) water molecules. These compounds differ in the type of M^+ as well as in the number of available donor and acceptor sites for H-bonds, which in turn is a function of the anion type present ($HTart^-$ or $Tart^{2-}$) and the water content.

The coordination number of M^+ is determined by its size (effective ionic radii: Li^+ 0.74, Na^+ 1.02, K^+ 1.38, Rb^+ 1.52 and Cs^+ 1.67 Å).[25] Thus, K^+, Rb^+ and Cs^+ can replace each other in certain packing arrangements with little effect on the anionic substructure (or anion + water substructure). This gives rise to several series of isostructures, M(L-HTart) (**16** – **18**),[26] M(D,L-HTart) (**2b**, **5**, **6**),[1a] LiM(D,L-Tart) · H_2O (**9** – **11**),[1b] NaM(L-Tart) · $4H_2O$ (**25**, **26**),[27] M_2(D or L-Tart) (**4**, **29**, **30**),[22] which can also extend to Tl^+ analogues (effective ionic radius 1.50 Å)[25] and ammonium analogues (where N–H···O bridges replace the alkali metal/oxygen bonds). In the M(L-HTart) series, the formation of mixed crystals was observed for the complete subset with M = K (**5**), Rb (**6**) and NH_4, but not for any combination with M = Cs (**2b**).[1a] Cs(L-HTart) is also the only compound of this series for which a second polymorph (**2a**) was obtained under the conditions of our study. Similarly, the Cs analogue **3** was the only dihydrate which, under the conditions of our study, was formed in addition to a monohydrate of the series[1b] LiM(D,L-Tart) · H_2O (M = K, Rb, Cs (**9** – **11**), NH_4). These observations illustrate that due to its size Cs^+ generally tends to prefer a higher coordination number than both K^+ and Rb^+.

The number of metal centers attached to an $HTart^-$ or $Tart^{2-}$ ligand and the number of coordinating O atoms per ligand both tend to increase with higher coordination numbers and decrease with higher water content. Connected MO_n polyhedra are typically linked into chains (16 structures). Isolated MO_x polyhedra are present only in Li(Li-HTart)[28] (**12**) and Na(Li-HTart)[29] (**14**), finite Li_2O_7 units are found in two Li_2Tart structures (**7**, **19a**)[1b, 28] and a Li_4O_{14} unit in **21**.[34] Examples of MO_n layers and frameworks occur exclusively in the $Tart^{2-}$ subset. The coordination polymer comprising linked metal centres, anions and (if present) water molecules is typically a three-dimensional framework. The only exceptions from this in Table 5 are Li(L-HTart) · H_2O (**13**) (chain)[30] and the two polymorphs of Na(D,L-HTart) · H_2O (**1a**, **b**) (layers).[19]

The anions and water molecules (if present) can be linked into an H-bonded chain, layer or framework structure, and there is no clear preference for either of these types. However, the anion/anion O–H···O=C interactions in this set of crystal structures are associated with a number of standard connectivity motifs, labelled **I** – **VII** (Fig. 7; Table 5, right-hand column).

All 13 structures of the $HTart^-$ subset of Table 5 display the $C_1^1(7)$ chain motif **I** which is based on a (carbonyl)O–H···O=C(carboxylate) bond between two $HTart^-$ ions. The chain motifs **II** and **III** can be present simultaneously in a crystal structure, or they can occur in combination with one of the four (hydroxyl)O–H···O=C bonded ring motifs (**IV** – **VII**). Non-adjacent H-bond donor and acceptor functions are employed in the $R_2^2(12)$ motif **IV**, while the analogous interactions involving adjacent functional groups yield the $R_2^2(10)$ ring motif **VI**. The $R_2^2(11)$ ring **V** connects one anion where the two H-bond functional groups

employed are adjacent to one another with one where they are not. The $R_2^1(7)$ ring **VII** results from a two-point (hydroxyl)O–H···O=C connection involving two hydroxyl groups of one anion and just one carboxylate group of another. For each motif, the number of occurrences in the $HTart^-$ and $Tart^{2-}$ subsets (h, t) is as follows: **I** (h = 13, t = 0), **II** (10, 14), **III** (8, 5), **IV** (2, 9), **V** (6, 0), **VI** (1, 1), **VII** (1, 2). The only two crystal structures of the entire set where neither of these seven motifs is present are Rochelle salt[27a] (**25**) and its isostructural Rb analogue[27b] (**26**).

Table 5. Characteristics of crystal structures of 35 alkali metal (M) hydrogen tartrates and tartrates. SpGr = space group, n_t/n_w = number of coordinating tartrate (t) and water (w) ligands at a metal centre, μ = number of metal centers attached to a ligand, κ = number of coordinating O atoms per ligand, D_I = dimensionality of structure formed by connected MO_n polyhedra, D_C = dimensionality of the coordination network, D_H = dimensionality of the O–H···O bonded structure.

Compound	M	#	CSD refcode	Ref.	SpGr	n_t/n_w	μ	κ	D_I	D_C	D_H	Motifs	
Li(L-HTart)		**12**	UNIROZ	28	$P2_1$	5	4	4	0[a]	3	3	**I, II, III**	
Li(L-HTart) · H_2O		**13**	YEKYIW	30	$P2_12_12_1$	4/1, 3/2	2,2	4,3	0[b]	1	2	**I, II**	
Na(L-HTart)		**14**	YELNIM	29	$P2_1$	6	6	6	0[a]	3	2	**I, II, III, VII**	
Na(L-HTart) · H_2O		**15**	ZZZSSS01	31	$P2_12_12_1$	7/1	4	5	1	3	1	**I**	
Na(D,L-HTart) · H_2O		**1a**	.	.	$P\bar{1}$	6/1	4	4	1	2	2	**I, IV**	
Na(D,L-HTart) · H_2O		**1b**	DULSIN	19	$P2_1/c$	6/1	4	4	1	2	2	**I, IV**	
M(L-HTart)	K	**16**	ZZZRZW01	26a	$P2_12_12_1$	8	7	5	1	3	2	**I, II, III, V**	[d]
	Rb	**17**	KAMBIJ	26b									
	Cs	**18**	CSHTAR10	26c									
M(D,L-HTart)	K	**5**	XAHZAI	1a	$P2_1/c$	8	7	5	1	3	2	**I, II, III, V**	[e]
	Rb	**6**	XAHZEM	1a									
	Cs	**2b**	XAHZIQ	1a									
Cs(D,L-HTart)		**2a**	.	.	$P\bar{1}$	9	7	6	1	3	3	**I, II, VI**	
Li_2(L-Tart)		**19a**	UNIRUF	28	$P2_12_12_1$	4	8	6	0[b]	3	1	**II, III, VII**	
Li_2(L-Tart)		**19b**	UNIRUF01	28	$C222_1$	4	6	6	1	3	1	**II, IV**	
Li_2(L-Tart)		**19c**	.	33	$C2$	4	8	6	1	3	1	**II, III, IV**	
Li_2(D,L-Tart)		**20a**	UNISIU	28	$C2/c$	4	8	6	1	3	1	**II, III, VII**	
Li_2(D,L-Tart)		**20b**	.	33	$P2_1/c$	4	8	6	1	3	1	**II**	
Li_2(D,L-Tart) · $2H_2O$		**21**	.	34	$P\bar{1}$	2/3	4	5	0[c]	2	2	**IV**	
Li_2(D,L-Tart) · $3H_2O$		**7**	CEGPEK	1b	$P2_1/c$	4/1, 1/3	3	5	0[b]	2	3	**II, III, IV**	[f]
LiNa(D,L-Tart) · $2H_2O$		**8**	CEGPIO	1b	$C2/c$	Li: 4/1 Na: 2/4	5	4	1	3	3	**III, IV**	
LiK(D-Tart) · H_2O		**22**	ZZZQMW01	35	$P2_12_12$	Li: 4/1 K: 6, 8/2	9	5	2	3	2	**II**	[g]
LiM(D,L-Tart) · H_2O	K	**9**	JEFVIA	1b	$C2/c$	Li:3/1 M: 6, 10	8	6	3	3	3	**IV**	[h]
	Rb	**10**	JEFVOG	1b									
	Cs	**11**	CEGPOU	1b									
LiCs(D,L-Tart) · $2H_2O$		**3**	.	.	$P2_1/c$	Li: 2/2 Cs: 6/3	6	5	2	3	1	**II, VI**	
Na_2(D-Tart) · $2H_2O$		**23**	NADTRT	38	$P2_12_12_1$	6, 4/2	8	6	1	3	2	**II**	[i]
Na_2(D,L-Tart)		**24**	COZGED	39	$Pbca$	6	7	6	3	3	2	**II**	
NaM(L-Tart) · $4H_2O$	K	**25**	KNATAR11[j,k]	27a	$P2_12_12$	Na: 3/3 M: 2/4, 4/4	5	4	2	3	3	.	[l]
	Rb	**26**	ZZZSVY01	27b									
NaK(D,L-Tart) · $3H_2O$		**27**	KEKXEF	44	$P2_1/n$	Na: 2/4 K: 6/2	6	6	2	3	3	**IV**	
K_2(L-Tart) · ½H_2O		**28**	ZZZLZE01	45	$I2$	6, 5/1	9	6	2	3	2	**II**	
M_2(D or L-Tart)	Rb	**29**	ZZZVZO02	22	$P3_121$ (D) $P3_221$ (L)	8	10	6	3	3	3	**II**	
	Cs	**30**	SOFJOM	22									
	$(Rb_{0.5}, Cs_{0.5})$	**4**	.	.									

[a] Isolated polyhedra.
[b] Pair of corner sharing tetrahedra.
[c] Li_4O_{14} units composed of four edge and corner sharing LiO_5 polyhedra
[d] Isostructural with the Tl and NH_4 analogues.[29, 32]
[e] Isostructural with the NH_4 analogue; formation of solid solutions for M = (K, Rb), (K, NH_4) and (Rb, NH_4.[1a]
[f] The crystal consists of alternating layers of the compositions $[Li_6(D,L\text{-}Tart)_3 \cdot 9H_2O]_n$ and $[Li_2(D,L\text{-}Tart) \cdot 3H_2O]_n$.
[g] Isostructural with the LiRb, LiTl and $LiNH_4$ analogues.[36]
[h] Isostructural with the NH_4Na analogue.[37]
[i] Reported as Na_2(D-Tart) · $2H_2O$; the structure model in the CSD is that of Na_2(L-Tart) · $2H_2O$.
[j] Paraelectric phase of Rochelle salt; phase transition to a ferroelectric monoclinic phase (KNATAR05)[40] between 255 and 297 K.
[k] A structure of the racemate, NaK(D,L-Tart) · $4H_2O$ (KNATDL01)[41] has not been included due to "abnormal geometrical features" reported by Sadanaga.[42]
[l] Isostructural with the $NaNH_4$ analogue.[43]

The program *XPac* was used to establish whether the presence of a common H-bond (connectivity) motif in certain crystal structures is also associated with packing (geometrical) similarity. If the position of the protonated carboxyl O atom (O*) is taken into consideration, the $HTart^-$ ion adopts either a geometry where the torsion angle C–C–C–O* is approximately +/–60° (type A) or one where it is near +/–120° (type B) (Fig. 7, top left). The A-type conformation is clearly more common, with Li(L-HTart) (**12**) and a 50% disorder component of **2a** being the only examples of the B-

type among the 13 relevant crystal structures listed in Table 5. Motif **I** implies that each $HTart^-$ ion has two (carbonyl)O–H···O=C(carboxylate) connection points to neighbouring anions. These lie either both on the same side ("*syn*") or on different sides ("*anti*") with respect to the plane defined by the four $HTart^-$ carbon atoms. Thus, four distinct (carbonyl)O–H···O=C(carboxylate) bonded chain types can arise from motif **I**, namely A-*syn* (present in **1a**, **1b**, **15**), A-*anti* (**2b**, **5**, **6**, **13**, **14**, **16** – **18**), B-*syn* (**2a**, **12**) and B-*anti* (**2a**). Except for **2a,** these chains have no symmetry other than translation.

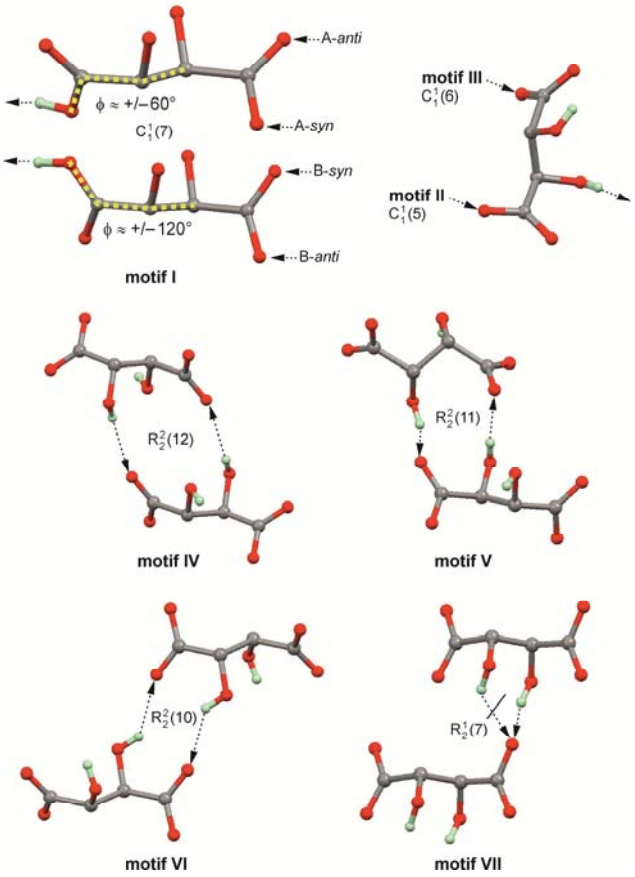

Fig. 7 Typical O–H···O=C interactions between anions of alkali metal $HTart^-$ and $Tart^{2-}$ salts.

All the motif **I** chains of the A-*syn* group are geometrically similar. Therefore, the crystal structures concerned exhibit a close one-dimensional packing similarity, evidenced by low dissimilarity indices *x* between 2.2 and 5.8 for the corresponding pairwise structure comparisons. Likewise, all the structures containing A-*anti* chains are 1D similar. Low dissimilarity indices were obtained for this set also (*x* = 1.2 – 4.3), except for the pairwise comparisons involving Na(L-HTart) (**14**), whose chain geometry deviates somewhat from the rest (*x* = 9.4 – 11.0). Each of these two principal chain geometries arising from motif **I** is associated with the packing of $HTart^-$ anions along a short crystallographic axis of characteristic length (A-*anti*: 7.594 – 7.692 Å; A-*syn*: 7.065 – 7.242 Å).

As discussed previously,[1a] the A-*anti* chain is also the basis for the close 2D packing relationship between the two sets of chiral and racemic hydrogen tartrates with *M* = K, Rb, Cs (**16** – **18** *vs*. **5**, **6,** **2b**) and NH_4. Furthermore, the packing relationship between the polymorphs **1a** and **1b** of Na(D,L-HTart) · H_2O discussed above (Fig. 2) is based on two A-*syn* strands, which are H-bonded to one another.

In the crystal structures of **2a**, **3**, **12**, **14**, **19a**, **19c, 20a**, **20b**, **23** and **28**, the H-bonded chains arising from motif **II** propagate along the shortest crystallographic axis (4.959 – 5.251 Å) with translation as their only symmetry operation. There are large variations in the geometry of these motif **II** chains, but relatively close 1D packing similarities exist within two subgroups, one comprising **2a**, **3** and **22** (*x* = 3.1 – 5.6) and the other **12**, **14**, **19a**, **20a** and **20b** (*x* = 1.9 – 11.5). Notable 2D packing similarity relationships based on motif **II** exist between **2a** and **3** (as discussed above, see Fig. 5) and between Li(L-HTart) (**12**) and Na(L-HTart) (**14**). Further details of the crystal packing comparisons can be found in the ESI†.

Conclusion

The crystal structures of the tartartes and hydrogen tartartes of alkali metals are based on a set of standard O–H···O=C-bond motifs (**I** – **VII**). These motifs are found in packing situations which, due to differences in the metal coordination geometry and water content, can differ considerably, resulting in the formation of specific MO_n structures, coordination polymers and hydrogen bond networks. These observations, combined with a lack of obvious alternatives, suggest that motifs **I** – **VII** are the universal motifs for the aggregation of $HTart^-$ and $Tart^{2-}$ ions in the solid state, even in salts of organic bases.

Of particular interest is the (carbonyl)O–H···O=C(carboxylate) bonded chain motif **I**, the universal connectivity mode for all *M*HTart salts in this study. The resulting chains can occur in four distinct subtypes, with types A-*anti* and A-*syn* dominating the investigated set. Each of these gives rise to a distinct series of crystal structures exhibiting 1D packing similarity which is typically associated with the packing along a short crystallographic axis. The CSD currently contains more than 180 crystal structures of hydrogen tartrate salts, and it would be very interesting to establish whether the same preferences are still valid for this larger set, especially in the presence of organic cations which often contain potential sites for hydrogen bonding. In this way, a general classification scheme of $HTart^-$ salts on the basis of 1D packing similarity relationships could be derived. This topic is currently being investigated in our laboratory and will be reported in a future publication.

Acknowledgements

We thank Susanne Coles and Eva Seeger for experimental assistance. M.B.H. thanks the Leverhulme Trust for the award of an Emeritus Fellowship. We thank the UK Engineering and Physical Science Research Council for support of the X-ray facilities at Southampton.

Notes and references

[a] *Institute of Pharmacy, University of Innsbruck, Innrain 52, 6020 Innsbruck, Austria. Fax: +43(0)512 507 5306 Tel: 43(0)5125075306; E-mail: thomas.gelbrich@uibk.ac.at*
[b] *School of Chemistry, University of Southampton, Highfield, Southampton, UK SO17 1BJ, UK. Fax: +44(0)2380596723; Tel: 44(0)2380594137; E-mail: m.b.hursthouse@soton.ac.uk*
[c] *Department of Chemistry, Faculty of Science, King Abdulaziz University, Jeddah, 21588, Saudi Arabia.*

† Electronic Supplementary Information (ESI) available: CCDC reference numbers 964976–9, analysis of structure similarity relationships and an overview of crystallisation experiments. For ESI and crystallographic data in CIF or other electronic format see DOI: 10.1039/b000000x/

‡ The program *XPac* can be obtained free of charge from the contact author.

1. (a) T. Gelbrich, T. L. Threlfall, S. Huth, E. Seeger and M. B. Hursthouse, *Z. Anorg. Allg. Chem.*, 2004, **630**, 1451-1458; (b) T. Gelbrich, T. L. Threlfall, S. Huth and E. Seeger, *Polyhedron*, 2006, **25**, 937-944.
2. S. R. Batten, S. M. Neville and D. R. Turner, *Coordination Polymers: Design, Analysis and Application*, RSC, Cambridge, 2009.
3. (a) K. Sumida, D. L. Rogow, J. A. Mason, T. M. McDonald, E. D. Bloch, Z. R. Herm, T.-H. Bae and J. R. Long, *Chem. Rev.*, 2011, **112**, 724-781; (b) T. A. Makal, J.-R. Li, W. Lu and H.-C. Zhou, *Chem. Soc. Rev.*, 2012, **41**, 7761-7779.
4. J.-R. Li, J. Sculley and H.-C. Zhou, *Chem. Rev.*, 2011, **112**, 869-932.
5. (a) D. Farrusseng, S. Aguado and C. Pinel, *Angew. Chem. Int. Ed.*, 2009, **48**, 7502-7513; (b) M. Yoon, R. Srirambalaji and K. Kim, *Chem. Rev.*, 2012, **112**, 1196-1231.
6. Y. Cui, Y. Yue, G. Qian and B. Chen, *Chem. Rev.*, 2012, **112**, 1126-1162.
7. J. J. Perry Iv, J. A. Perman and M. J. Zaworotko, *Chemical Society Reviews*, 2009, **38**, 1400-1417.
8. (a) K. M. Fromm, *Coordination Chemistry Reviews*, 2008, **252**, 856-885; (b) D. Banerjee and J. B. Parise, *Cryst. Growth Des.*, 2011, **11**, 4704-4720.
9. R. Hooft, *COLLECT: Data Collection and Processing Software*, 1998, Nonius B.V.
10. DirAx: A. J. M. Duisenberg, *J. Appl. Cryst.*, 1992, **25**, 92-96.
11. DENZO: Z. Otwinowski and W. Minor, in *Methods in Enzymology: Macromolecular Crystallography, part A*, eds. C. W. Carter, Jr and R. M. Sweet, Academic Press, New York, 1997, vol. 276, pp. 307–326.
12. G. M. Sheldrick, *SADABS. Version 2007/7*, 2007, Bruker AXS Inc., Madison, Wisconsin, USA.
13. G. M. Sheldrick, *Acta Crystallogr., Sect. A: Fundam. Crystallogr.*, 2008, **64**, 112-122.
14. T. Gelbrich and M. B. Hursthouse, *CrystEngComm*, 2005, **7**, 324-336.
15. T. Gelbrich, T. L. Threlfall and M. B. Hursthouse, *CrystEngComm*, 2012, **14**, 5454-5464.
16. V. A. Blatov, *Compcomm*, 2006, **7**, 4-38.
17. I. A. Baburin and V. A. Blatov, *Acta Crystallogr., Sect. B: Struct. Sci.*, 2007, **63**, 791-802.
18. (a) M. C. Etter, J. C. MacDonald and J. Bernstein, *Acta Crystallogr., Sect. B: Struct. Sci.*, 1990, **46**, 256-262; (b) J. Bernstein, R. E. Davis, L. Shimoni and N.-L. Chang, *Angew. Chem. Int. Ed.*, 1995, **34**, 1555-1573.
19. M. T. M. Al-Dajani, H. H. Abdallah, N. Mohamed, C. K. Quah and H.-K. Fun, *Acta Crystallogr., Sect. E.: Struct Rep. Online*, 2010, **66**, m138-m139.
20. T. Gelbrich, T. L. Threlfall and M. B. Hursthouse, *Acta Crystallogr., Sect. C: Cryst. Struct. Commun.*, 2012, **68**, o421-o426.
21. (a) V. A. Blatov, L. Carlucci, G. Ciani and D. M. Proserpio, *CrystEngComm*, 2004, **6**, 378-395; (b) N. L. Rosi, J. Kim, M. Eddaoudi, B. Chen, M. O'Keeffe and O. M. Yaghi, *J. Am. Chem. Soc.*, 2005, **127**, 1504-1518.
22. K. Stadnicka and Z. Brożek, *Acta Crystallogr., Sect. B: Struct. Sci.*, 1991, **47**, 484-492.
23. (a) O. Delgado Friedrichs, M. O'Keeffe and O. M. Yaghi, *Acta Crystallogr., Sect. A: Fundam. Crystallogr.*, 2003, **59**, 515-525; (b) O. Delgado Friedrichs, M. O'Keeffe and O. M. Yaghi, *Solid State Sciences*, 2003, **5**, 73-78.
24. F. H. Allen, *Acta Crystallogr., Sect. B: Struct. Sci.*, 2002, **58**, 380-388.
25. R. Shannon, *Acta Crystallogr., Sect. A: Fundam. Crystallogr.*, 1976, **32**, 751-767.
26. (a) J. Buschmann and P. Luger, *Acta Crystallogr., Sect. C: Cryst. Struct. Commun.*, 1985, **41**, 206-208; (b) L. K. Templeton and D. H. Templeton, *Acta Crystallogr., Sect. C: Cryst. Struct. Commun.*, 1989, **45**, 675-676; (c) L. K. Templeton and D. H. Templeton, *Acta Crystallogr., Sect. A: Fundam. Crystallogr.*, 1978, **34**, 368-371.
27. (a) C. H. Görbitz and E. Sagstuen, *Acta Crystallogr., Sect. E.: Struct Rep. Online*, 2008, **64**, m507-m508; (b) M. Lutz and A. M. M. Schreurs, *Acta Crystallogr., Sect. C: Cryst. Struct. Commun.*, 2008, **64**, m296-m299.
28. H. H. M. Yeung, M. Kosa, M. Parrinello, P. M. Forster and A. K. Cheetham, *Cryst. Growth Des.*, 2011, **11**, 221-230.
29. R. C. Bott, G. Smith, D. S. Sagatys, D. E. Lynch, A. N. Reddy and H. L. Kennard, *Z. Kristallogr.*, 1994, **209**, 803-807.
30. R. C. Bott, D. S. Sagatys, G. Smith, K. A. Byriel and C. H. L. Kennard, *Polyhedron*, 1994, **13**, 3135-3141.
31. R. C. Bott, D. S. Sagatys, D. E. Lynch, G. Smith and C. H. L. Kennard, *Acta Crystallogr., Sect. C: Cryst. Struct. Commun.*, 1993, **49**, 1150-1152.
32. A. Spek, *Acta Crystallogr., Sect. C: Cryst. Struct. Commun.*, 1987, **43**, 1633-1634.
33. H. H.-M. Yeung, M. Kosa, M. Parrinello and A. K. Cheetham, *Cryst. Growth Des.*, 2013, **13**, 3705-3715.
34. H. H.-M. Yeung and A. K. Cheetham, *Dalton Trans.*, 2014, **43**, 95-102.
35. C. Ottenz, M. Schürmann, H. Preut and Bleckmann, *Zeitschrift für Kristallographie - New Crystal Structures* 1998, **213**, 166.
36. (a) G. Shirane, F. Jona and R. Pepinsky, *Proc. I.R.E.*, 1955, **43**, 1738-1793; (b) M. I. Kay, *Ferroelectrics*, 1978, **19**, 159-164; (c) H. Hinazumi and T. Mitsui, *Acta Crystallogr., Sect. B: Struct. Sci.*, 1972, **28**, 3299-3305.
37. Z. Brożek, D. Mucha and K. Stadnicka, *Acta Crystallogr., Sect. B: Struct. Sci.*, 1994, **50**, 465-472.
38. G. K. Ambady and G. Kartha, *Acta Crystallogr., Sect. B: Struct. Sci.*, 1968, **24**, 1540-1547.

39. W. Arbuckle, S. Cartner, A. R. Kennedy and C. A. Morrison, *Acta Crystallogr., Sect. E.: Struct Rep. Online*, 2009, **65**, m1232.
40. X. Solans, C. Gonzalez-Silgo and C. Ruiz-Pérez, *J. Solid State Chem.*, 1997, **131**, 350-357.
41. R. Sadanaga, *Acta Crystallogr.*, 1950, **3**, 416-423.
42. J. Clark, *Acta Crystallogr.*, 1964, **17**, 459-461.
43. Z. Brożek and K. Stadnicka, *Acta Crystallogr., Sect. B: Struct. Sci.*, 1994, **50**, 59-68.
44. A. E. Egorova, V. A. Ivanov, N. V. Somov, V. N. Portnov and E. V. Chuprunov, *Crystallogr. Rep.*, 2011, **56**, 1038-1041.
45. R. Boese, D. Bläser, R. Latz and M. Piennisch, *Acta Crystallogr., Sect. C: Cryst. Struct. Commun.*, 1995, **51**, 2227-2229.